NASA

National Aeronautics and
Space Administration

NASA CR-165434

INTERLAMINAR CRACK GROWTH IN FIBER REINFORCED COMPOSITES DURING FATIGUE

Final Report - Part III

by

S.S. Wang and H.T. Wang

Department of Theoretical and Applied Mechanics
UNIVERSITY OF ILLINOIS
at Urbana-Champaign

prepared for

NATIONAL AERONAUTICS AND SPACE ADMINISTRATION

NASA Lewis Research Center
Grant NSG 3044

1. Report No.	2. Government Accession No.	3. Recipient's Catalog No.
NASA CR-165434		

4. Title and Subtitle	5. Report Date
Interlaminar Crack Growth in Fiber Reinforced Composites During Fatigue	February 1981
	6. Performing Organization Code

7. Author(s)	8. Performing Organization Report No.
S. S. Wang and H. T. Wang	
	10. Work Unit No.

9. Performing Organization Name and Address	11. Contract or Grant No.
University of Illinois Urbana, IL 61801	NSG 3044
	13. Type of Report and Period Covered

12. Sponsoring Agency Name and Address	Final Report - Part III
National Aeronautics and Space Administration Washington DC 20546	14. Sponsoring Agency Code

15. Supplementary Notes

Project Manager: C. C. Chamis
NASA Lewis Research Center, Structures & Mechanical Technologies Division
21000 Brookpark Road, Mail Stop 49-6
Cleveland, OH 44135

16. Abstract

Interlaminar crack growth behavior in fiber-reinforced composites subjected to fatigue loading was investigated experimentally and theoretically. In the experimental phase of the study, interlaminar crack propagation rates and mechanisms were determined for the cases of various geometries, laminate parameters and cyclic stress levels. An advanced singular hybrid-stress finite element method was used in conjunction with the experimental results to examine the local crack-tip behavior and to characterize the crack propagation during fatigue. Results elucidate the basic nature of the cyclic delamination damage, and relate the interlaminar crack growth rate to the range of mixed-mode crack-tip stress intensity factors. The results show that crack growth rates to be related directly to the range of the mixed-mode cyclic stress intensity factors by a power law relationship.

17. Key Words (Suggested by Author(s))	18. Distribution Statement
fiber composites, stress intensity, mix-mode, crack growth, hybrid element, stress analysis, finite element, experiments	Unclassified, Unlimited

19. Security Classif. (of this report)	20. Security Classif. (of this page)	21. No. of Pages	22. Price*
Unclassified	Unclassified		

* For sale by the National Technical Information Service, Springfield, Virginia 22161

TABLE OF CONTENTS

FOREWORD

This report descirbes a portion of the results obtained on NASA Grant NSG 3044. This work was done under subcontract to the University of Illinois, Urbana, with Prof. S.S. Wang as the Principal Investigator. The prime grantee was the Massachusetts Institute of Technology, with Prof. F.J. McGarry as the Principal Investigator and Dr. J.F. Mandell as a major participant. The NASA - LeRC Project Manager was Dr. C.C. Chamis.

Efforts in this project are primarily directed towards the development of finite element analyses for the study of flaw growth and fracture of fiber composites. This report presents analytical and experimental results for delamination crack growth in fatigue. The work is a follow-up to an earlier interim report NASA CR-135248. H.T. Wang was a research assistant at M.I.T. when the experimental work was performed.

Abstract

This paper presents an investigation of interlaminar crack growth behavior in fiber-reinforced composites subjected to fatigue loading. In the experimental phase of the study, interlaminar crack propagation rates and mechanisms were determined for the cases of various geometries, laminate parameters and cyclic stress levels. An advanced singular hybrid-stress finite element method was used in conjunction with the experimental results to examine the local crack-tip behavior and to characterize the crack propagation during fatigue. Results elucidate the basic nature of the cyclic delamination damage, and relate the interlaminar crack growth rate to the range of mixed-mode crack-tip stress intensity factors. The study provides fundamental insight into the problem, reveals several important features of the interlaminar fatigue failure, and should be of practical importance in selection, testing and design of composite materials.

INTRODUCTION

Damage tolerance has been of great concern for the structural reliability and integrity of fiber-reinforced composites in their advanced engineering applications. Interlaminar cracking, sometimes also called delamination, is considered one of the most frequently encountered types of damage occurring in the material subjected to fatigue loading. It is commonly initiated at geometric discontinuities, processing and manufacturing defects, machining and service flaws, and takes the form of separation of plies under mechanical, thermal and/or environmental loading. The presence and growth of an interlaminar crack may result in (1) significant reduction of stiffness, (2) exposure of the interior to adverse environmental attack, and the degradation of the composite, which may lead to the final failure of the structure. Thus, understanding the interlaminar crack growth behavior under cyclic stresses is of fundamental importance in the application of composite materials.

Laminated composites generally consist of a number of plies with different fiber orientations separated by resin-rich interlaminar regions as shown in Fig. 1. The interlaminar region usually has a dimension of one twentieth to one tenth of the individual ply thickness, depending on manufacturing and processing methods. Since the strength is usually low and stresses are high in the interlaminar region, almost all kinds of defects such as voids, inclusions, broken plies, etc., unavoidably tend to grow in an interlaminar mode at very low nominal stress levels and to propagate along preferential paths. This phenomenon is unique to composites and is particularly significant when the materials are subjected to cyclic loading. The development of a through-the-thickness crack from a defect or flaw in a

real composite may be difficult in many cases. This is in contrast to the flaw growth behavior in monolithic metals in which defects usually develop into a through-the-thickness crack during fatigue.

The importance of the fatigue delamination has long been recognized, but research progress has been slow, since this kind of real-life defect is characteristically difficult to study due to the inherent complexities of the crack geometry, the material anisotropy and discontinuity, and the crack-tip singularity. Because of the matrix-dominated and localized fracture behavior of the delamination, it would be unwise to make any simplification which fails to consider the important resin-rich interlaminar region. Numerous studies have been conducted to investigate the initiation of an interlaminar crack in composites caused by geometric discontinuities [1-3]*, processing and manufacturing defects [4, 5] . Relatively little work concerning the interlaminar crack growth behavior has been reported [6, 7], especially that associated with in-service and manufacturing defects under repeated stresses. This paper presents an experimental and analytical investigation of the crack growth behavior of an interlaminar crack initiated from a service-induced surface notch in a composite laminate subjected to cyclic loading. Unidirectional composites, which have the simplest laminate configuration, are examined first to explore the fundamental nature of the interlaminar crack. Interlaminar fatigue failure behavior of more complicated angle-ply composites is then studied and compared with the results obtained from the basic unidirectional fiber configuration.

---

*Numbers in brackets designate References at end of paper.

EXPERIMENTAL PROGRAM

One of the central concepts in this experimental program is to develop a suitable test technique in which stable interlaminar crack growth can be obtained under cyclic fatigue without being affected by the complex three-dimensional edge effect [8]. Experiments were conducted to identify the influential geometric and laminate parameters, to examine the interlaminar failure mechanisms, and to characterize rationally the fatigue damage behavior in the composites. They also helped to establish a realistic mechanical model for later analytical study and provided experimental data to validate the results.

Materials and Specimen Preparation

Scotchply Type 1003 E-glass/epoxy (manufactured by 3M Company, Minneapolis, Minn.) was used in the fabrication of all test specimens. The material was received in a unidirectional prepreg form. Test composites were made by a compressive molding process following manufacturer's instructions. Specimens used in the study were eight-ply composite laminates of various fiber orientations and stacking sequences. An interlaminar crack initiator was introduced in the form of a surface notch penetrating one or more plies as desired by cutting individual plies with a razor blade, prior to the laminate assembly. The specimen had a gauge length of six inches and a width of one inch, and the surface notch extended completely across the specimen width as shown in Fig. 2.

Experimental Procedures

All interlaminar crack growth tests were conducted at room temperature in a laboratory environment. Fatigue experiments were run on an Instron

Model 1211 dynamic cycler. Specimens were cycled under a controlled sinusoidal load-time condition with a minimum tensile stress of 1.0 ksi and some maximum tension at a frequency of approximately 5 cycles per second (Fig. 3). No significant heating of the specimen was observed at this frequency during the test. A traveling optical microscope mounted on the testing facilities was used periodically to monitor the interlaminar crack extension in the specimen under transmitted light and to measure accurately the delamination crack length after a given number of cycles. Fatigue crack growth data were obtained for several cases in which interlaminar cracks were initiated at different depths under the surface. Experimental results, expressed by delamination length versus number of loading cycles, are reported in the next section.

Advantages of Present Test Method

The present experimental method has several advantages particularly suitable for studying the cyclic interlaminar crack growth behavior in composites. As mentioned previously, the initiation of delamination from geometric discontinuities is complicated by the three-dimensional edge effect. Thus, the growth of the interlaminar crack may be expected to be influenced also by the edges of the laminate. Better appreciation of the nature of the problem can be obtained by investigating the delamination growth by itself without being affected by geometric boundaries. This purpose may be achieved in the current experiments by using specimens wide enough to minimize the localized edge effect on the propagating interlaminar crack front. The experiment can also provide a controlled, stable delamination growth at a desired depth and enables the crack length

to be measured accurately and conveniently. Moreover, the specimen geometry is considered relatively easy to model in the analytic study, which will be discussed in the next section.

ANALYTICAL APPROACH

The current analytical approach, using an advanced singular finite-element method of the hybrid-stress model, has a capability to overcome the aforementioned difficulties and can provide a numerically exact solution for the problem. The method, pioneered by Pian et al. [9], gives a rapid rate of solution convergence and enables an accurate description of the crack-tip response by introducing a crack-tip superelement including singular and higher order terms based on the complex variable formulation of Muskhelishvili stress functions. It is particularly suitable for studying crack problems in composites, since the complex crack geometry, laminate properties and traction boundary conditions of crack surfaces can be exactly modeled. Additional features of the method include the flexibility of formulation, the selection of element characteristics, and the expedient achievement of interelement compatibility.

Mechanical Model and Assumptions

Microscopic observation in the experimental study indicated that interlaminar crack growth is clearly a matrix-dominated progressive failure mechanism occurring in a resin-rich interlaminar region. Thus, the composite laminate is modeled as an assembly of anisotropic plies bonded together by thin resin interlayers subjected to an in-plane cyclic stress. Each fiber

reinforced lamina of thickness t_0 has its material axis oriented from the loading direction by an angle θ_i. The resin-rich interlayer is assumed to have a uniform thickness, t_1, and perfectly bonded with the plies everywhere except the region where a crack is initiated from the surface notch tip. The crack geometry and laminate configuration are conveniently expressed by $(\underline{\theta_1/\theta_2}/\!/\,\theta_3/\theta_4/\theta_5/\ldots\ldots)$, where the double slash and the underline represent the location of the interlaminar crack and the penetration depth of the surface notch, respectively. The interlaminar crack is modeled, for simplicity without losing generality, as a flaw completely embedded in a resin-rich interlayer as shown in Fig. 4. Studies on other extreme cases such as the crack located at a vanishing interlayer or at a ply/interlayer interface, giving a more complicated oscillating three-dimensional singular stresses, are reported elsewhere [10].

Method of Analysis

General procedure of formulating the plane crack problem in the composite is described in this section. Details of the formulation for the crack-tip superelement and surrounding non-singular elements have been given elsewhere [11, 12] and are not repeated here. Briefly, the formulation of the analysis is based on the variational principle of modified complementary energy. Following Muskhelishvili's formulation [13], the stress and displacement fields may be expressed in terms of two stress functions, $\phi(z)$ and $\psi(z)$, of a complex variable z. A mapping function $w(\xi)$ is then introduced to transfer the singular crack domain to a ξ-plane by $z = w(\xi) = \xi^2$ where $-\pi/2 \leq \arg \xi \leq \pi/2$. The functions $\phi(\xi)$ and $\psi(\xi)$ are analytical and interrelated by the traction boundary condition along crack surfaces.

In the crack-tip superelement formulation, $\phi(\xi)$ is assumed to have the form

$$\phi(\xi) = \sum_{1}^{n} b_j \, \xi^j \tag{1}$$

and function $\psi(\xi)$ may be obtained as

$$\psi(\xi) = - \sum_{1}^{n} [\bar{b}_j (-1)^j + \frac{1}{2} j \, b_j] \, \xi^j \tag{2}$$

where $$b_j = \beta_j + i \, \beta_{n+j} \quad \text{(non-symmetric case)} \tag{3}$$

or $$b_j = \beta_j \quad \text{(symmetric case)} \tag{4}$$

and βs are real constants to be determined. Using Eqs. 1 and 2, the stress and displacement fields may be expressed in terms of the stress coefficients βs. The boundary traction $\underset{\sim}{T}$ can be calculated by

$$T_i = \sigma_{ij} \, \nu_j \tag{5}$$

Interpolating boundary displacements $\tilde{u}$ in terms of nodal displacements $\tilde{q}$ and inserting $\underset{\sim}{\sigma}$ and $\underset{\sim}{T}$ into the variational principle, the crack-tip superelement stiffness matrix may be obtained.

Surrounding non-singular element stiffness matrices are formulated by a conventional hybrid-stress finite element method through a minimum complementary energy principle [14]. The anisotropic elastic properties of each glass/epoxy lamina are considered in the analysis by introducing an appropriate compliance matrix in the element stiffness formulation. Since boundary displacement functions are independently assumed for the crack element and non-singular elements, interelement compatibility can be ensured by a suitable choice of interpolation functions.

The assembled governing equations for the whole system may be written as

$$\underset{\sim\sim}{K} \underset{\sim}{q} = \underset{\sim}{Q} \tag{6}$$

where $\underset{\sim}{K}$ is the global stiffness matrix, and $\underset{\sim}{Q}$, the consistent loading vector. After solving $\underset{\sim}{q}$ from Eq. 6 by an appropriate solution scheme, the stress and strain fields can be determined. Stress intensity factors K_I and K_{II} corresponding to an applied stress level and an interlaminar crack length may be found from the relation

$$K_I = \sqrt{2\pi}\ \beta_1 \tag{7}$$

and

$$K_{II} = \sqrt{2\pi}\ \beta_{n+1} \tag{8}$$

The associated elastic energy release rates G_I and G_{II} can be obtained by a standard procedure.

The accuracy and convergence assessments of the solutions are complicated by several unusual features of the problem and of the method of analysis due to the inherently singular nature of the interlaminar crack. A study of the accuracy and convergence of the analysis, and solution stability has been conducted by testing cases for which independent solutions are available. Excellent agreements with existing closed-form solutions were obtained. The results indicated that accuracy within approximately one percent of the converged solutions of K_I and K_{II} can be achieved by the optimum mesh arrangements used in the current study. Details of the study were reported in [12].

For the cases of cyclic loading, the ranges of interlaminar crack-tip stress intensity factors, ΔK_I and ΔK_{II}, may be determined by

$$\Delta K_I = (K_I)_{max} - (K_I)_{min} \tag{9}$$

and

$$\Delta K_{II} = (K_{II})_{max} - (K_{II})_{min} \tag{10}$$

where $(K_I)_{max}$ and $(K_{II})_{max}$ are opening and shearing mode stress intensity

factors corresponding to a maximum cyclic stress level σ_{max} for the delamination crack of length ℓ_d, and $(K_I)_{min}$ and $(K_{II})_{min}$ are the values associated with a minimum cyclic stress level σ_{min}. Numerical results of $(K_I)_{max}$, $(K_{II})_{max}$, $(K_I)_{min}$ and $(K_{II})_{min}$ were accurately computed for the delamination test specimens by the computer-aided numerical method.

RESULTS AND DISCUSSION

Typical results of the crack growth study of the eight-ply fiberglass composites subjected to nominal cyclic stresses are presented in this section. In the experimental phase, interlaminar crack growth rates were determined by the constant load-amplitude fatigue tests. In the analytical phase of the study, the crack-tip stress field and the ranges of the cyclic stress intensity factors were obtained for the laminates with various geometric and ply configurations. Interlaminar crack growth rates during fatigue were then characterized by the ranges of the mixed-mode cyclic stress intensity factors. The individual glass/epoxy lamina used in the analytical modeling had a thickness dimension of 0.01 inch, and the interlaminar layer was taken as one-twentieth of the ply thickness as observed in the microscope. Elastic constants for each lamina were given by

$E_{LL} = 5.0 \times 10^6$ psi $\qquad G_{Lz} = 0.75 \times 10^6$ psi

$E_{zz} = 1.5 \times 10^6$ psi $\qquad \nu_{Lz} = 0.25$

The interlaminar epoxy resin phase has the properties:

$E_m = 0.5 \times 10^6$ psi $\qquad \nu_m = 0.35$

$G_m = 0.185 \times 10^6$ psi

Interlaminar Crack Growth During Fatigue

Microscopic observation in the fatigue experiments revealed that delamination was initiated after a few load cycles. It propagated in a stable manner and was clearly a matrix-dominated, progressive failure mechanism occuring in a resin-rich region between plies. This suggested an appropriate mechanical model used later in the analytical study. Measurements were made on the change of the subcritical crack length during cyclic loading. Typical fatigue crack growth data in unidirectional and $(\pm 45°)_{4s}$ glass/epoxy composites are presented in Figs. 5 and 6. Test results shown in the figures for several maximum cyclic stress levels indicate that crack lengths change drastically with the number of load cycles and that crack growth rates are very distinct between the unidirectional and angle-ply laminates. The growth rates of the delamination $d\ell_d/dN$ were determined by a computational procedure based on the first derivatives of crack growth curves fitted by experimental data. The crack extension rates were found to increase continuously during the course of fatigue, and rapid crack propagation occurred when the ultimate delamination resistance of the composite was approached. Intralaminar failure, which may lead to a complete fracture of the composites, were often observed in (45°/-45°// 45°/-45°/-45°/45°/-45°/45°) and quasi-isotropic (45°/-45°// 0°/90°/90°/0°/-45°/45°) glass/epoxy prior to large-scale delamination. The number of loading cycles to fracture versus applied cyclic stress for the two composite systems is shown in Fig. 7. The ultimate static strengths (σ_{UTS}) of these laminates were 14.7 and 44.55 Ksi, respectively.

Interlaminar Crack-Tip Response

The driving force of the interlaminar crack growth depends primarily on local crack-tip stresses. Thus, it is necessary to have accurate information on the crack-tip behavior. Since the geometry and material properties are very complex in the problem, the response of the composite to the damage may be best illustrated by isostress contours. These contours were plotted from the analytical solutions obtained by the aforementioned hybrid finite element analysis. Figure 8 gives the distribution of the in-plane stress $\sigma_{xx}/\sigma_{\infty}$ around the crack with ℓ_d = 0.8 inch in a ($\underline{0°/0°}$// 0°/0°/0°/0°/0°/0°) glass/epoxy. The computer plot provides a graphic description of the solutions and an overall view of the damage behavior. It reveals several salient features of the problem: (i) the intensified stress field caused by interlaminar damage is very localized within the matrix-rich interlaminar region ahead of the crack tip, (ii) a large stress gradient exists through the laminate thickness with high concentration in adjacent plies, and (iii) a local compressive in-plane stress component is developed along the lower crack flank. Figures 9 and 10 show the contour plots of interlaminar shear and transverse normal stress distributions in the near field. Both stress components reach extremely high levels within the thin interlaminar region when the crack tip is approached. The interlaminar stresses extend continuously through the interface into the adjacent plies.

A more accurate description of the near field stresses may be expressed by a log σ_{ij} versus log r representation, where r is the distance ahead of the crack tip. The numerical results near the crack tip give straight lines with a slope of $-\frac{1}{2}$, indicating a classical fracture mechanics solution, i.e., a $1/\sqrt{r}$ singularity; details of the results may be found in [15]. The opening

and shearing mode stress components are observed to have the same order of magnitude at the interlaminar crack tip when a uniaxial nominal stress is applied. The singular stress domain is rather small and is embedded in the resin-rich interlayer region.

The redistribution of laminate stresses due to the propagating interlaminar crack will have a significant effect on the deformation and fracture of the composite. For example, the compressive stress in the lower crack flank may introduce severe local buckling of the delaminated plies in the vicinity of the surface notch. This phenomenon was experimentally observed in [16,17]. The highly nonuniform stress distributions in the transverse direction shown in the isostress contour plots suggest that the classical laminate theory may not be applicable to a delaminated composite. The stress concentration may also introduce a transition from interlaminar to intralaminar fracture mode when different ply orientations are used [18]. Furthermore, the presence of the interlaminar crack may become detrimental to the serviceability of the material when used in an adverse environment such as mositure and corrosive chemicals, because not only does the crack expose the interior of the composite to environmental attack, but also the stress concentration in the near field may enhance the rate-dependent degradation process, which is evident by the results in [19].

Fatigue Crack Growth Rate Characterization

The stable extension of an interlaminar crack in glass/epoxy composites reveal several features of the progressive interlaminar fatigue damage, which can be used to probe the nature of the delamination growth behavior. Since the interlaminar crack growth is observed as a matrix-dominated failure process and since it is strongly affected by the local crack-tip response, it may be appropriate to postulate, as in the cases of metals and polymers[20,21],

that ΔK_I and ΔK_{II} are critical controlling factors in the fatigue damage. The ranges of the cyclic stress intensity factors are, in turn, related to the crack length, the cyclic stress, the geometry and laminate properties. In the current fatigue test, stress intensity factors change continuously as the load and the interlaminar crack length increase, and the corresponding crack growth rate varies accordingly. For a given crack length and laminate configuration, exact stress intensity factors may be computed by using the present analytical method. Therefore, ΔK_I and ΔK_{II} can be precisely determined from Eqs. 9 and 10. It may be reasonable, at this point, to postulate further that ΔK_I and ΔK_{II} independently affect the interlaminar crack growth rate. Thus, $d\ell_d/dN$, obtained from the experiments, may be related to both the ΔK_I and the ΔK_{II} simultaneously as shown in Figs. 11 and 12 for the glass/epoxy composites with two distinct ply orientations. Strong correlation between $d\ell_d/dN$ and ΔKs is observed from the results, and a power law relationship of the following form may be established,

$$\frac{\log\left(\frac{d\ell_d}{dN}\right)}{\alpha_1} = \frac{\log(\Delta K_I) + C_1}{\alpha_2} = \frac{\log(\Delta K_{II}) + C_2}{\alpha_3} \tag{11}$$

where α_is are the directional cosines of the lines determined by a least-square curve-fitting method, and C_1 and C_2 are constants associated with the threshold values of the mixed-mode stress intensity factor ranges. This functional relationship in Eq. 11 suggests that

$$\frac{d\ell_d}{dN} \sim (\Delta K_I)^{\lambda_1} \tag{12a}$$

or

$$\frac{d\ell_d}{dN} \sim (\Delta K_{II})^{\lambda_2} \tag{12b}$$

where the exponents λ_1 and λ_2 are related to the laminate configuration, the crack geometry and the material properties of composites. The results in

Figs. 11 and 12 give respective λ_1 and λ_2 the values of 7.32 and 7.42, for 0° and 7.52 and 7.74 for $\pm$ 45°. The strong correlation between the interlaminar crack propagation rate and the ranges of cyclic stress intensity factors are very informative. Further study is needed to identify the nature of the interlaminar crack under more complex fatigue loading and to construct the crack growth rate surface of mixed-mode failure so as to characterize fully the interlaminar fatigue behavior, and the relative dominance of each individual fracture mode.

Limitations of Current Study

It should be noted here that several geometric and material complications in composites have not been included in the current analytical modeling, such as the nonuniformity of the resin-rich interlaminar region thickness, the heterogeneity of the fiber and matrix phases, and other types of commonly encountered defects (e.g. voids, inclusions, broken plies, etc.). These complications are statistical in nature and almost always exist in the material. Their presence may have significant effects on the interlaminar crack growth behavior, but has not been fully explored yet. The anti-plane mode deformation and fracture (mode III), which may have an important contribution to the progressive fatigue failure of the materials, especially in the angle-plied composite laminates, have not been considered in the present study. A recent study on edge delimination [10] reveals that the mode III component of the crack-tip field has a very high value, which may be primarily responsible for the interlaminar crack growth and failure of the composites, including the $\pm$ 45° case. Furthermore, residual stresses due to ply differential thermal contraction during the curing process may strongly affect the crack growth behavior. This effect has not been included in the present investigation.

SUMMARY AND CONCLUSION

A combined experimental and analytical investigation of interlaminar crack growth in fiber-reinforced composites under cyclic loading has been presented. The unidirectional ply configuration was studied first to elucidate the fundamental failure behavior and, later, served as a reference for studying more complex angle-ply composite laminates. In the experimental phase, microscopic observation of failure mechanisms revealed that delamination is clearly a matrix-dominated, progressive failure occurring in the resin-rich interlaminar region. Interlaminar crack growth rates under tension-tension fatigue were obtained, and test results were further used in conjunction with analytical characterization. The analytical study of the problem was based on an advanced hybrid-stress finite element method, formulated by using Muskhelishvili's complex stress functions through a modified complementary energy principle. Numerical solutions clarify the basic nature of the cyclic interlaminar failure. Implications of the results in the applicability of classical laminate theory to the delamination problem due to the localized interlaminar crack-tip singularity and the stress concentration in the adjacent plies were discussed. Fatigue crack growth rates were found to be related directly to the ranges of the mixed-mode cyclic stress intensity factors by a power law relationship. The study elucidates many important features of the delamination problem, provides insight into the interlaminar fatigue behavior, and should be of practical importance in the testing and design of composites materials.

Acknowledgments

The work described in this paper was supported in part by NASA-Lewis Research Center, Cleveland, Ohio under Grant NSG 3044. The authors are grateful to Dr. C. C. Chamis for his encouragement and cooperation. Fruitful discussion with Dr. J. F. Mandell of the Massachusetts Institute of Technology is deeply acknowledged.

REFERENCES

1 Pipes, R. B., Kaminski, B. E. and Pagano, N. J., "Influence of the Free Edge upon the Strength of Angle-Ply Laminates," *Analysis of the Test Methods for High Modulus Fibers and Composites*, *ASTM STP 521*, American Society for Testing and Materials, 1973, pp. 218-228.

2 Wang, S. S., Mandell, J. F. and McGarry, F. J., "Three Dimensional Solution for a Through-Thickness Crack with Crack Tip Damage in a Cross-Plied Laminate," *Fracture Mechanics of Composites*, *ASTM STP 593*, American Society for Testing and Materials, 1975, pp. 61-85.

3 Reifsnider, K. L., Henneke, E. G., II and Stinchcomb, W. W., "Delamination in Quasi-isotropic Graphite-Epoxy Laminates," *Composite Materials: Testing and Design (Fourth Conference)*, *ASTM STP 617*, American Society for Testing and Materials, 1977, pp. 93-105.

4 Verett, R. M. and Demuts, E., "Effects of Manufacturing and In-Service Defects on Composite Materials," *Proceedings of the Army Symposium on Solid Mechanics, 1976-Composite Materials: The Influence of Mechanics of Failure on Design*, AMMRC MS 76-72, Army Mechanics and Materials Research Center, Watertown, Mass., 1976, pp. 123-137.

5 Wang, S. S., "Delamination Fracture from Surface Notch in $(\pm 45°/0°/90°)_s$ Graphite/Epoxy Composites," *Proceedings of the Second International Conference on Composite Materials (ICCM-II)*, TMS-AIME, 1978.

6 Erdogan, F. and Arin, K., "A Sandwich Plate with a Part-Through and Debonding Crack," *Engineering Fracture Mechanics*, Vol. 4, 1972, pp. 449-458.

7 Kulkarni, S. V. and Frederick, D., "Propagation of Delamination in a Layered Cylindrical Shell," *International Journal of Fracture*, Vol. 9, 1973, pp. 113-115.

8 Pipes, R. B. and Pagano, N. J., "Interlaminar Stresses in Composite Laminates under Uniform Axial Extension," *Journal of Composite Materials*, Vol. 4, 1970, pp. 538-548.

9 Pian, T. H. H., Tong, P. and Luk, C. H., "Elastic Crack Analysis by a Finite Element Method," *Proceedings of the Third Conference on Matrix Methods in Structural Mechanics*, 1971, pp. 661-682.

10 Wang, S. S., "An Analysis of Edge Delamination Crack in Composite Laminate under Uniform Axial Extension," NASA CR-165439, National Aeronautics and Space Administration, Washington, D.C., 1981.

11 Tong, P., Pian, T. H. H. and Lasry, S., "A Hybrid-Element Approach to Crack Problems in Plane Elasticity," *International Journal for Numerical Methods in Engineering*, Vol. 7, 1973, pp. 297-308.

12 Wang, S. S., Mandell, J. F. and McGarry, F. J., "An Analysis of the Crack Tip Stress Field in DCB Adhesive Fracture Specimens," *International Journal of Fracture*, Vol. 14, No. 1, Feb., 1978, pp. 39-58.

13 Muskhelishvili, N. I., *Some Basic Problems of Mathematical Theory of Elasticity*, P. Noordhoff, Groningen, The Netherlands, 1953.

14 Pian, T. H. H., "Derivation of Element Stiffness Matrix by Assumed Stress Distribution," *American Institute of Aeronautics and Astronautics Journal*, Vol. 2, 1964, pp. 1333-1336.

15 Wang, S. S. and Mandell, J. F., "Analysis of Delamination in Unidirectional and Crossplied Fiber Reinforced Composites Containing Surface Cracks," NASA Technical Report NASA-CR-135248, May, 1977.

16 Sendeckyj, G. P., Stalnaker, H. D., Kleismit, R. A., "Effect of Temperature on Frequency Response of Surface-Notched $[(0^{o}, \pm 45^{o}, 0^{o})_{s}]_{3}$ Graphite-Epoxy Laminate", *Fatigue of Filamentary Composite Materials, ASTM STP* 636, K. L. Reifsnider and K. N. Lauraitis, Eds., American Society for Testing and Materials, 1977, pp. 123-140.

17 Sendeckyj, G. P., "Surface Notches in Composites", submitted for publication, Air Force Flight Dynamics Laboratory, Wright-Patterson AFB, Ohio, 1978.

18 Wang, S. S., "Failure Modes of Interlaminar Crack in Quasi-isotropic Fiber-Reinforced Composites Containing a Surface Notch," in *Failure Modes and Processing of Composites IV,* TMS-AIME, Oct., 1977.

19 Mandell, J. F., "Origin of Moisture Effects on Crack Propagation in Composites," Research Report R77-4, Department of Materials Science and Engineering, M.I.T., Dec., 1977.

20 Hertzberg, R. W., in *Deformation and Fracture Mechanics of Engineering Materials,* Chap. 13, John Wiley and Sons, Inc., New York, 1976, pp. 465-520.

21 Manson, J. A. and Hertzberg, R. W., "Fatigue Failure in Polymers," *Critical Reviews in Macromolecular Science,* Vol. 1, No. 4, 1973, pp. 433-500.

LIST OF CAPTIONS FOR FIGURES

Fig. 1 Micrograph of Graphite Fiber Reinforced Composite Showing Individual Plies and Resin-Rich Interlayers Between Plies

Fig. 2 Fatigue Test Specimen for Interlaminar Crack Growth Study

Fig. 3 Stress vs. Time During Fatigue Test

Fig. 4 Interlaminar Crack Geometry, Coordinate System, and Hybrid-Stress F.E.M. Mesh Configuration in Composites

Fig. 5 Interlaminar Crack Growth During Fatigue in (0°/0°// 0°/0°/ 0°/0°/0°/0°) Glass/Epoxy

Fig. 6 Interlaminar Crack Growth During Fatigue in (45°/-45°// 45°/ -45°/-45°/45°/-45°/45°) Glass/Epoxy

Fig. 7 Fatigue Stress vs. Number of Cycles to Failure for Glass/ Epoxy Composites with Different Laminate Configurations

Fig. 8 In-plane Longitudinal Stress Contours $\sigma_{xx}/\sigma_\infty$ Near Interlaminar Crack Tip in (0°/0°// 0°/0°/0°/0°/0°/0°) Glass/ Epoxy

Fig. 9 Transverse Normal Stress Contours $\sigma_{zz}/\sigma_\infty$ Near Interlaminar Crack Tip in (0°/0°// 0°/0°/0°/0°/0°/0°) Glass/Epoxy

Fig. 10 Interlaminar Shear Stress Contours $\sigma_{xz}/\sigma_\infty$ Near Interlaminar Crack Tip in (0°/0°// 0°/0°/0°/0°/0°/0°) Glass/Epoxy

Fig. 11 Interlaminar Crack Growth Rate $d\ell_d/dN$ as a Function of the Ranges of Mixed-Mode Stress Intensity Factors, ΔK_I and ΔK_{II} for (0°/0°// 0°/0°/0°/0°/0°/0°) Glass/Epoxy

Fig. 12 Interlaminar Crack Growth Rate $d\ell_d/dN$ as a Function of the Ranges of Mixed-Mode Stress Intensity Factors ΔK_I and ΔK_{II} for (45°/-45°// 45°/-45°/-45°/45°/-45°/45°) Glass/Epoxy

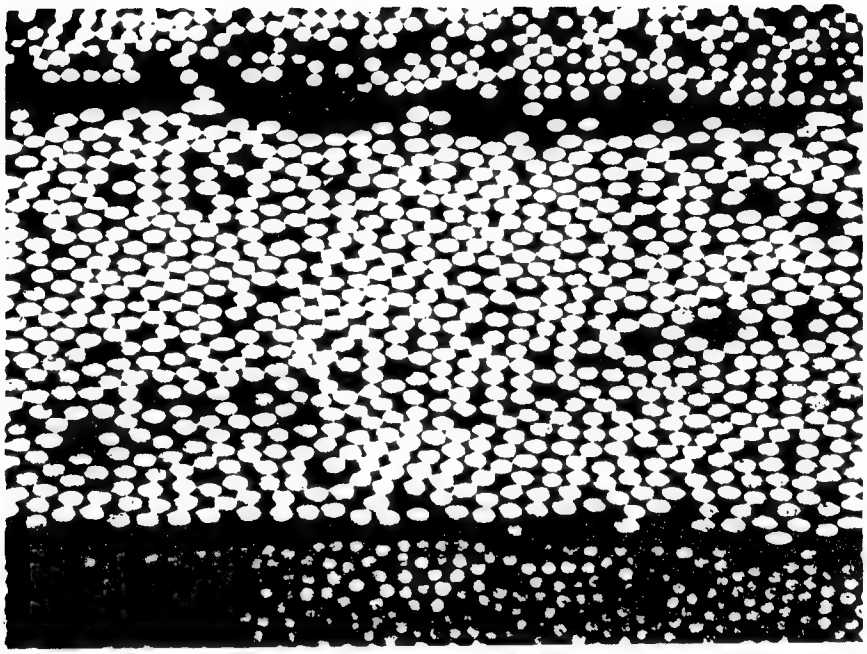

FIG. 1 MICROGRAPH OF GRAPHITE FIBER REINFORCED COMPOSITE SHOWING INDIVIDUAL PLIES AND RESIN-RICH INTERLAYERS BETWEEN PLIES.

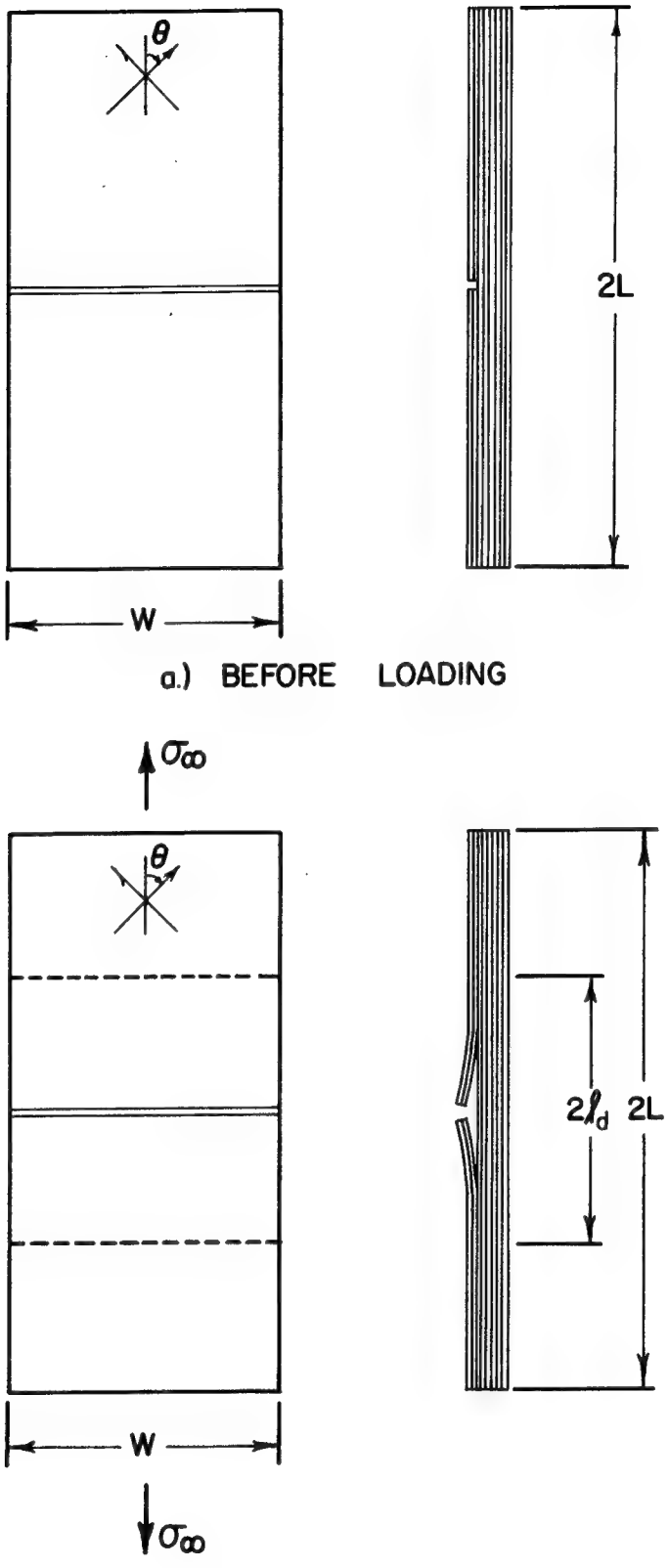

FIG. 2 FATIGUE TEST SPECIMEN FOR INTERLAMINAR CRACK GROWTH STUDY (2L = 6.0 in.; W = 1.0 in.)

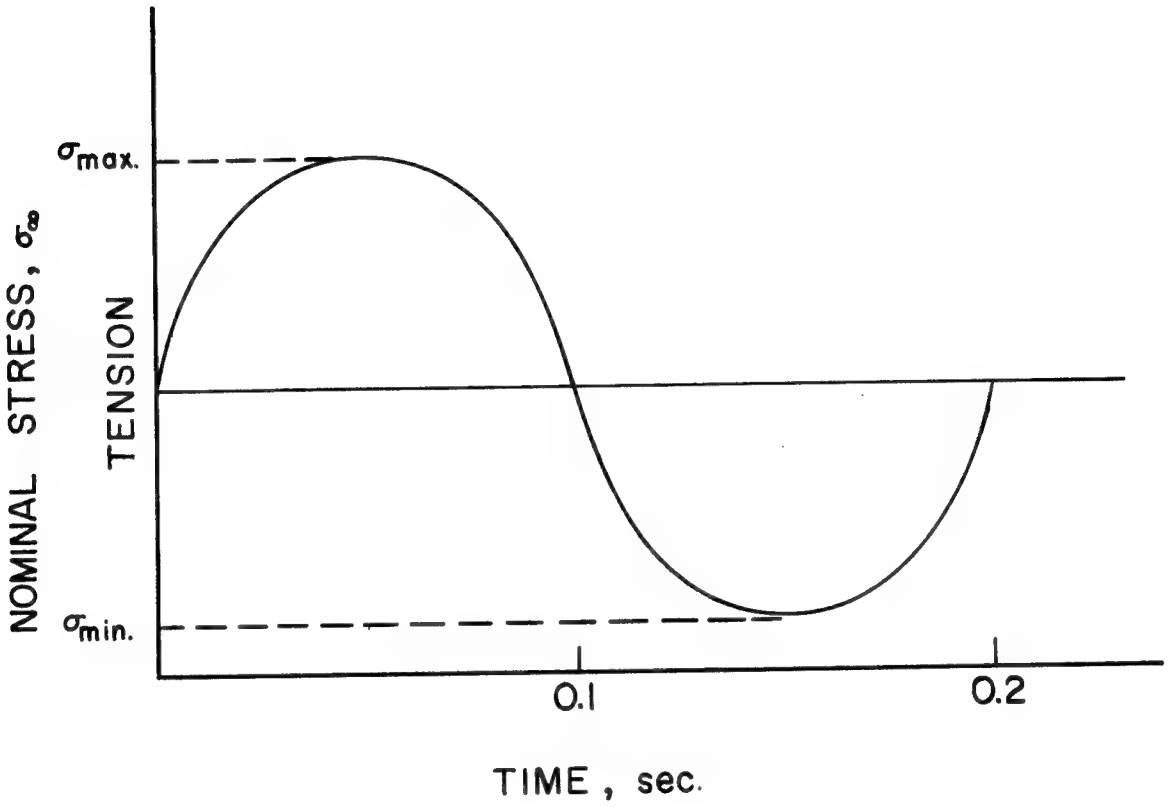

FIG. 3 STRESS vs. TIME FOR FATIGUE TEST

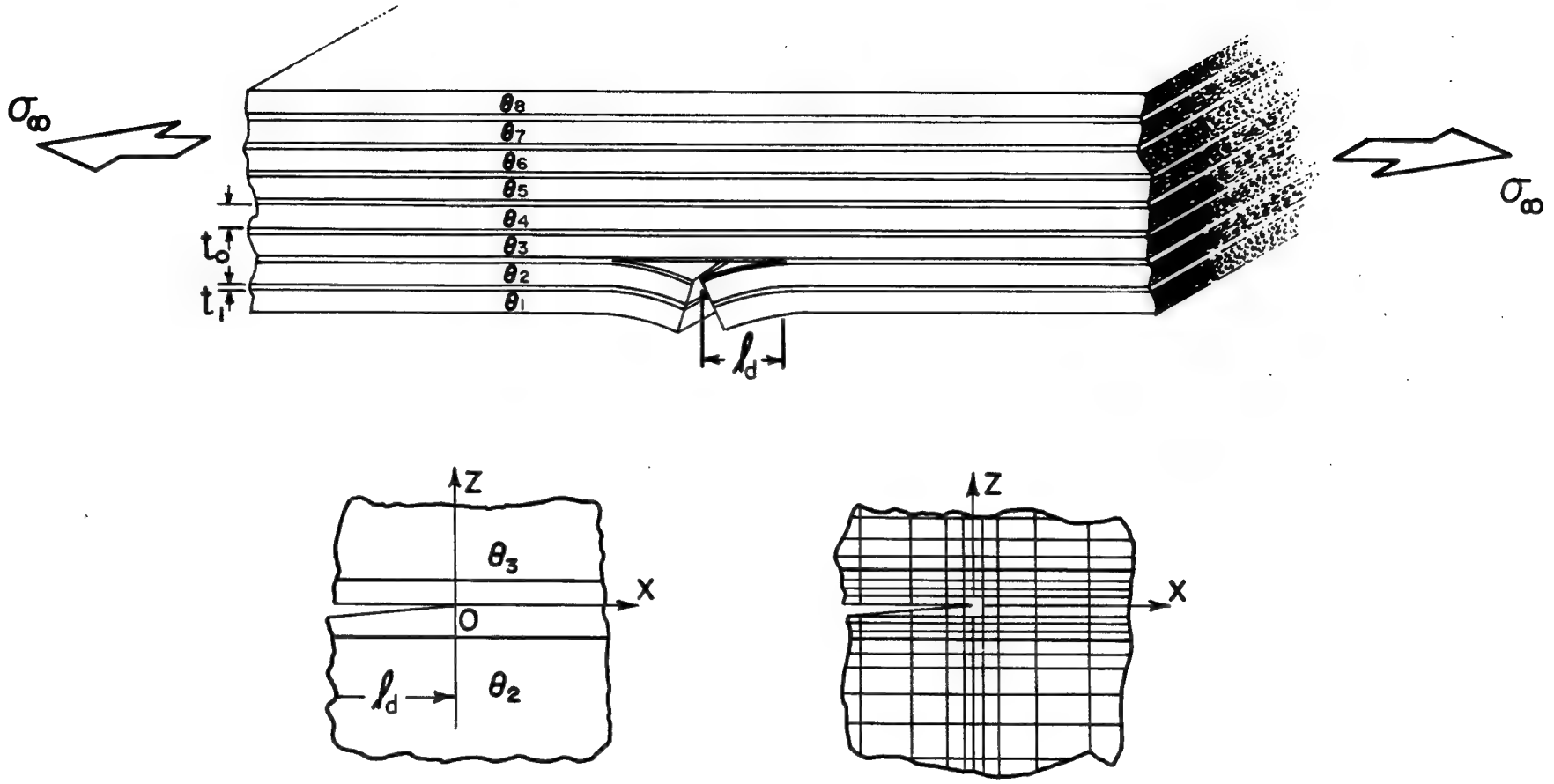

FIG. 4 INTERLAMINAR CRACK GEOMETRY, COORDINATE SYSTEM AND HYBRID-STRESS F.E.M. MESH CONFIGURATION IN COMPOSITES

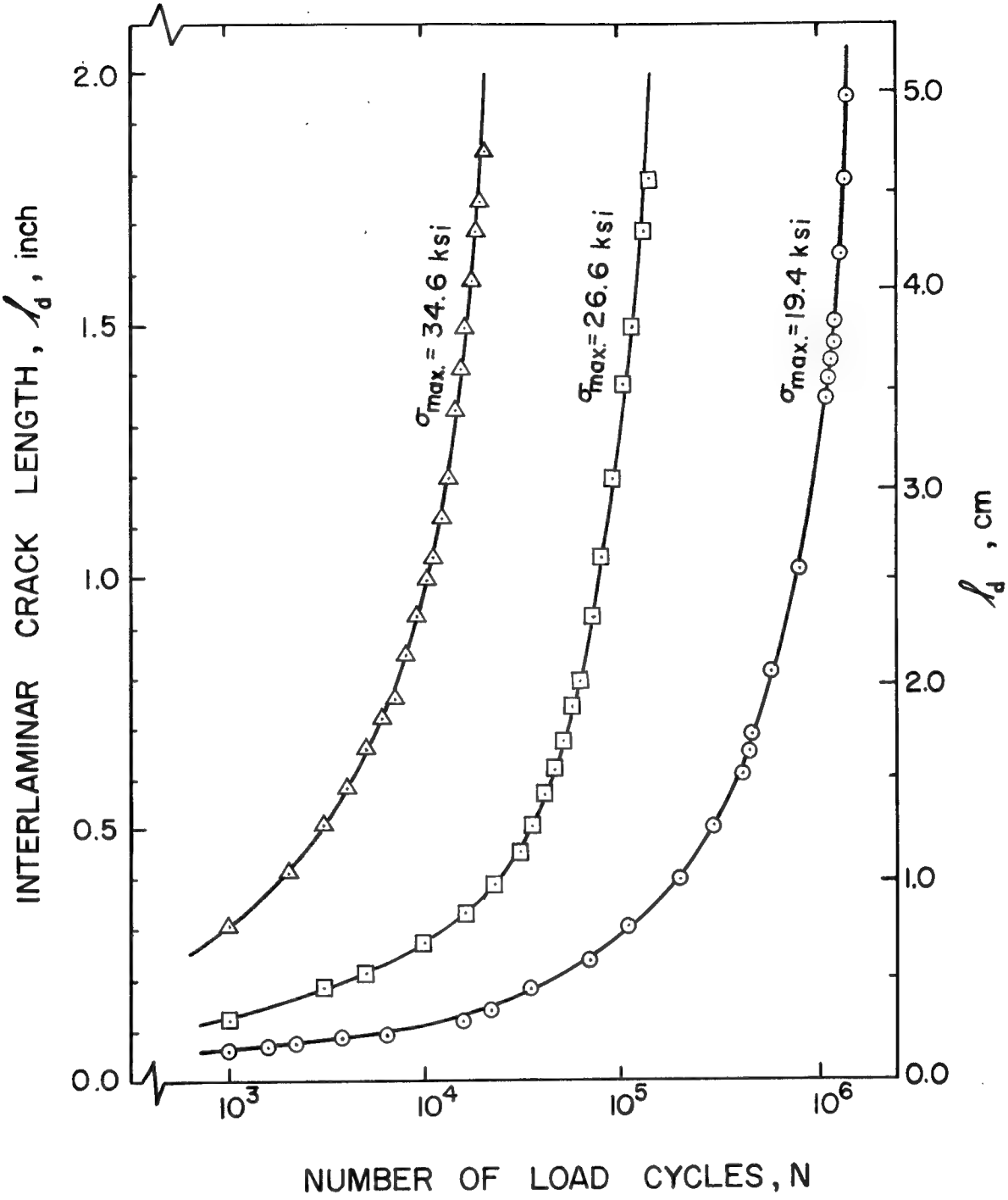

FIG. 5 INTERLAMINAR CRACK GROWTH DURING FATIGUE IN (0%0%/0%/0%/0%/0%/0%/0°) GLASS/EPOXY

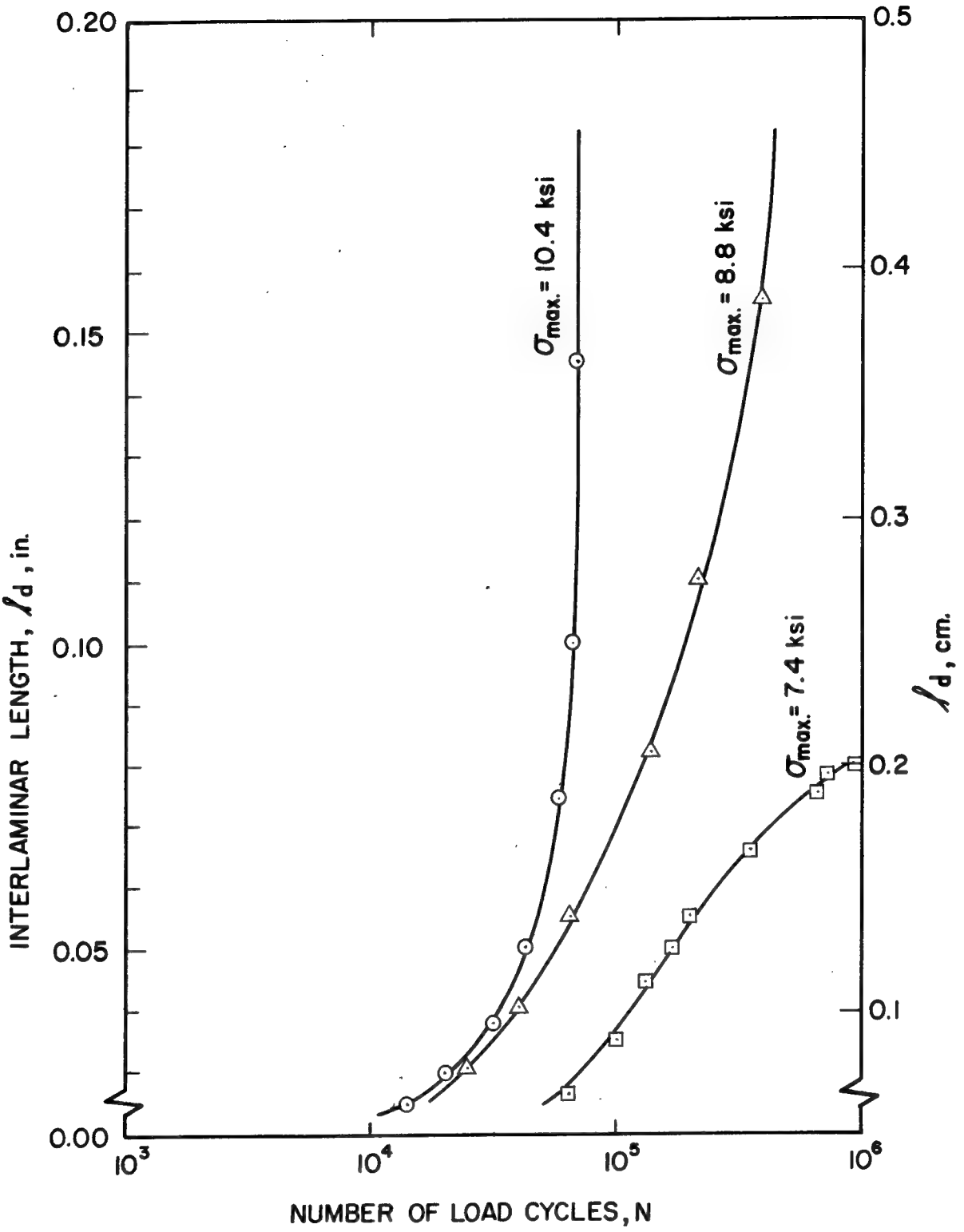

FIG. 6 INTERLAMINAR CRACK GROWTH DURING FATIGUE IN (45%-45%//45%-45%-45%/45%-45%/45°) GLASS/EPOXY

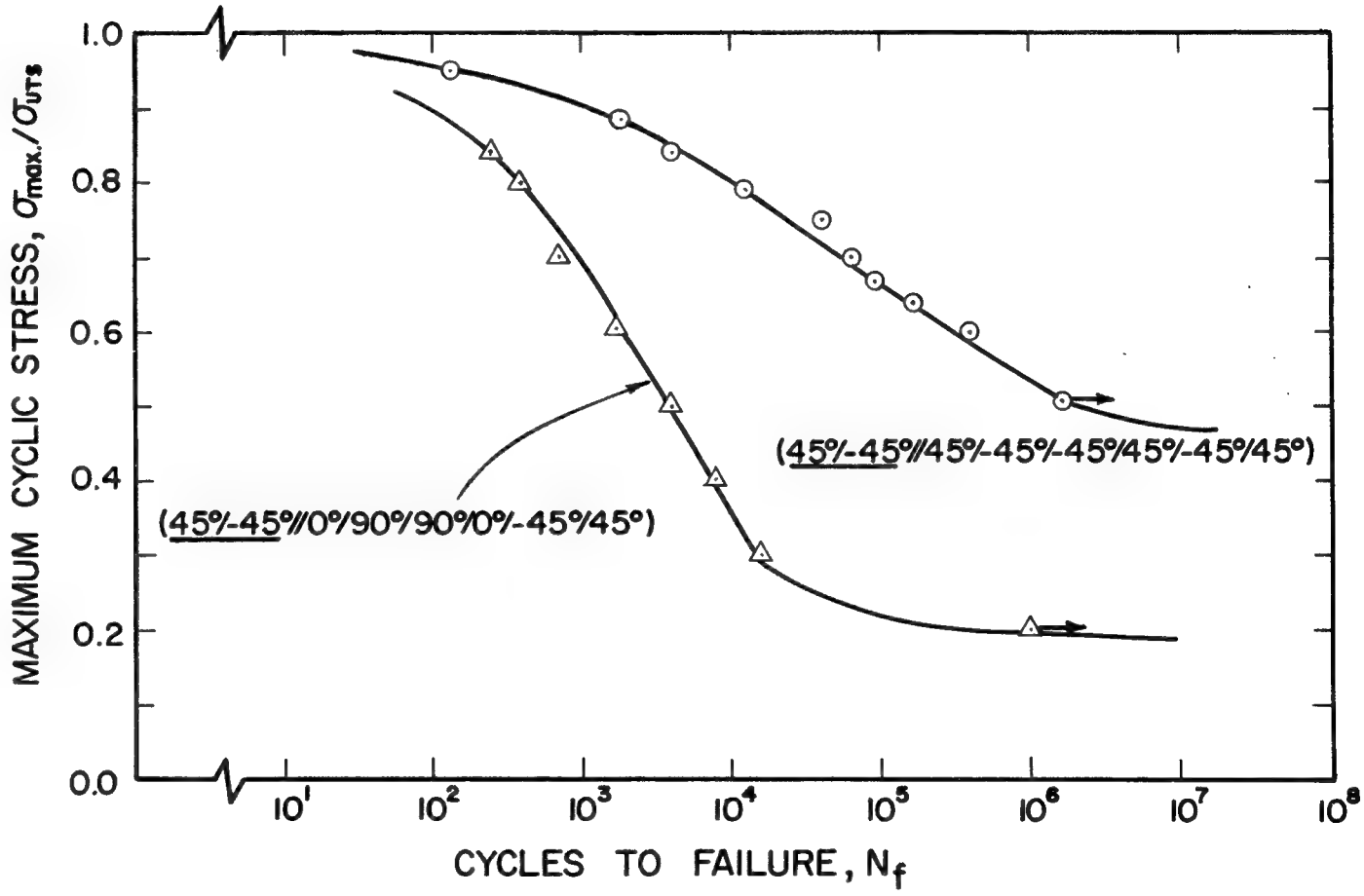

FIG. 7 FATIGUE STRESS vs NUMBER OF CYCLES TO FAILURE FOR GLASS/EPOXY COMPOSITES WITH DIFFERENT LAMINATE CONFIGURATIONS

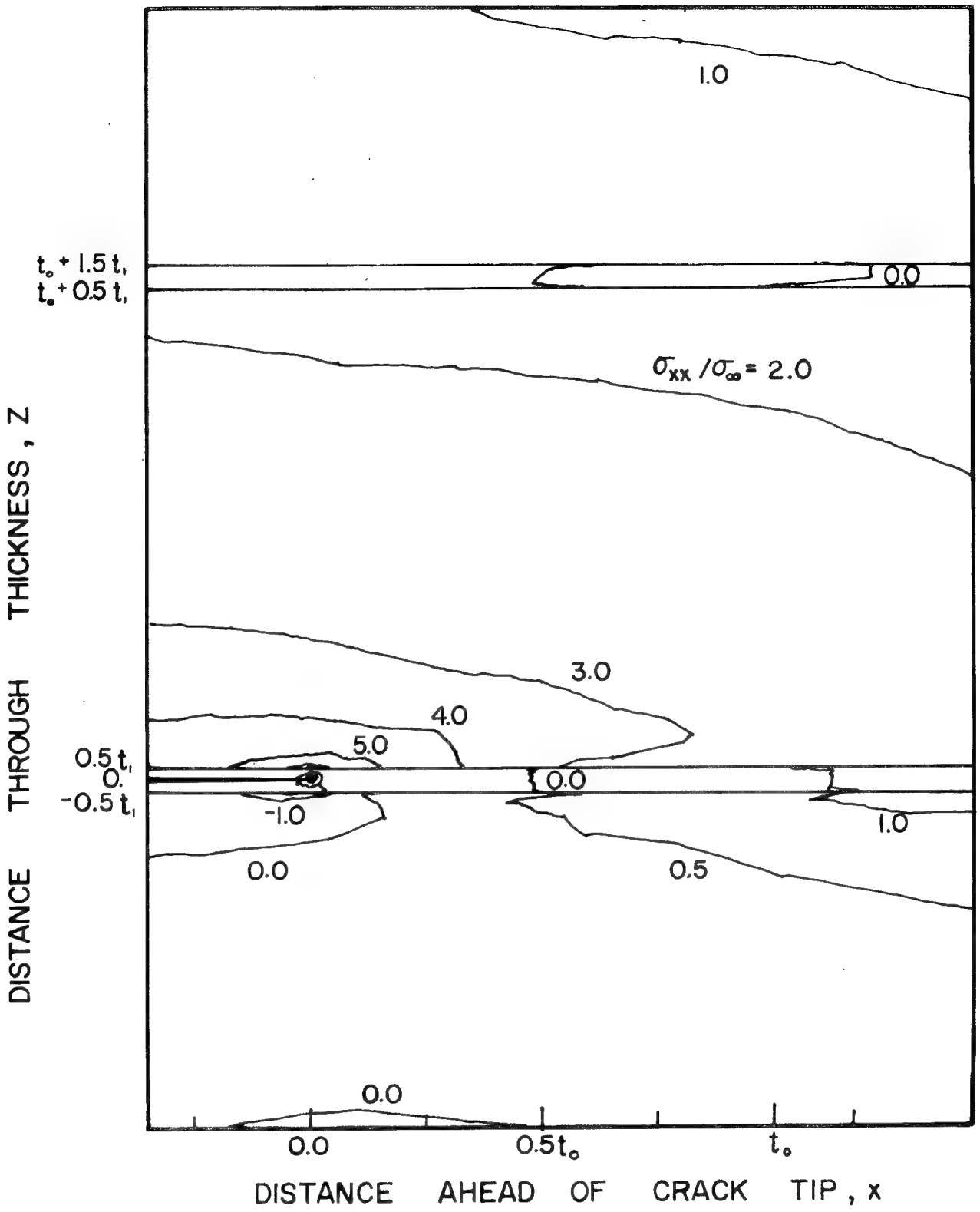

FIG. 8 IN-PLANE LONGITUDINAL STRESS CONTOUR $\sigma_{xx}/\sigma_\infty$ NEAR INTERLAMINAR CRACK TIP IN (0%0%/0%/0%/0%/0%/0%/0°) GLASS / EPOXY

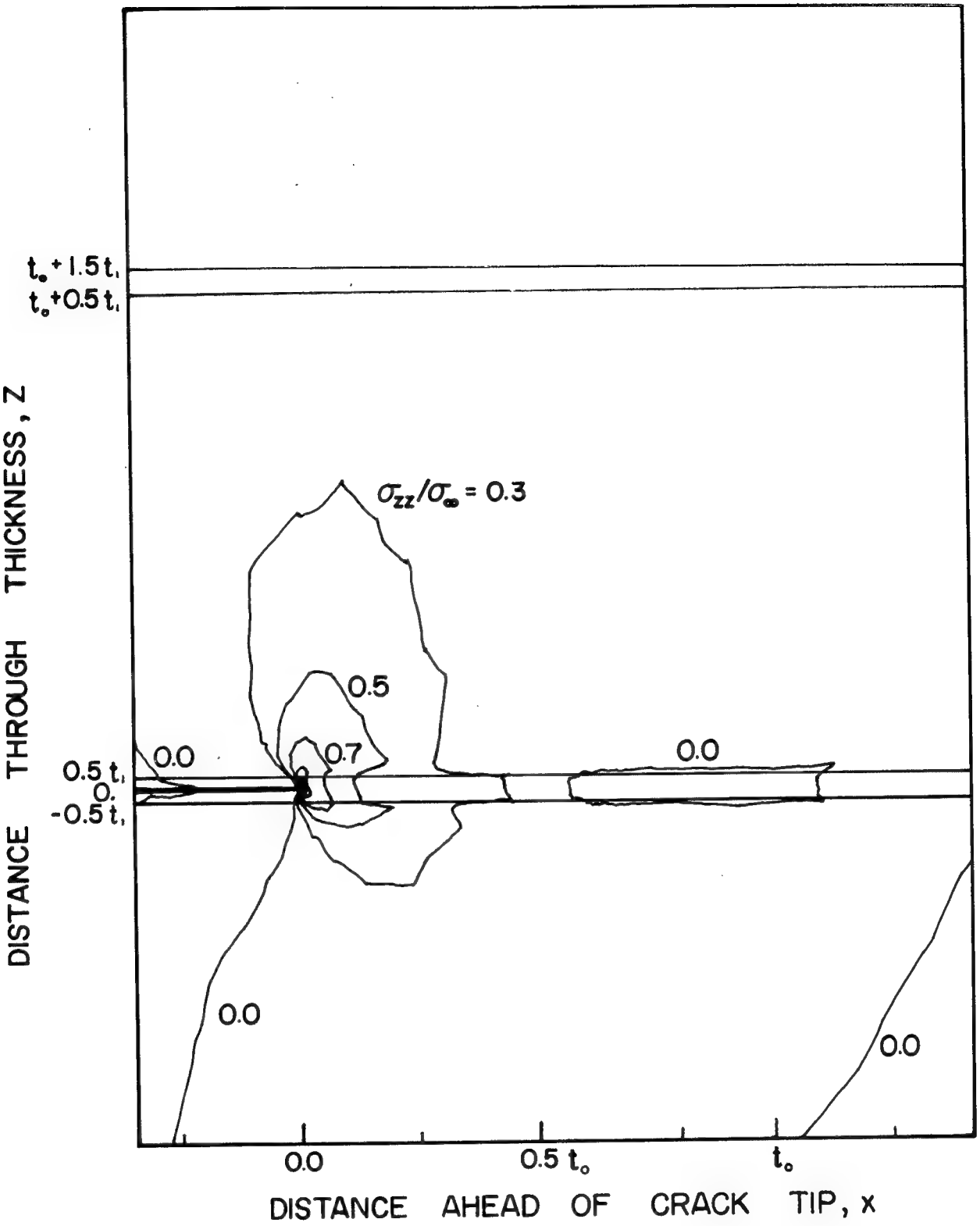

FIG. 9 TRANSVERSE NORMAL STRESS CONTOURS $\sigma_{zz}/\sigma_\infty$ NEAR INTERLAMINAR CRACK TIP IN (0%0%/0%0%0%0%0%0°) GLASS / EPOXY

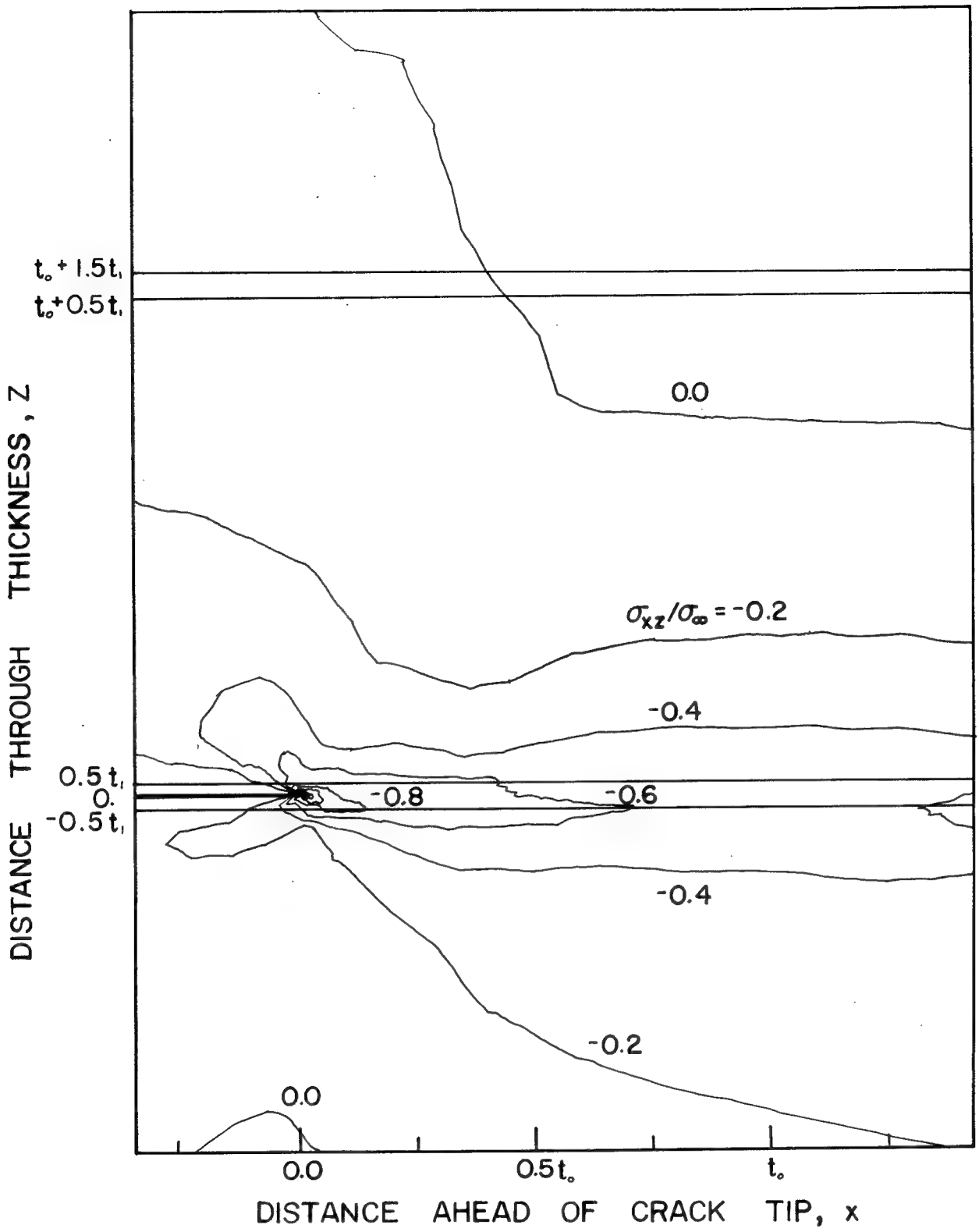

FIG. 10 INTERLAMINAR SHEAR STRESS CONTOURS $\sigma_{xz}/\sigma_\infty$ NEAR INTERLAMINAR CRACK TIP IN (0%0%/0%/0%/0%/0%/0%/0°) GLASS/EPOXY

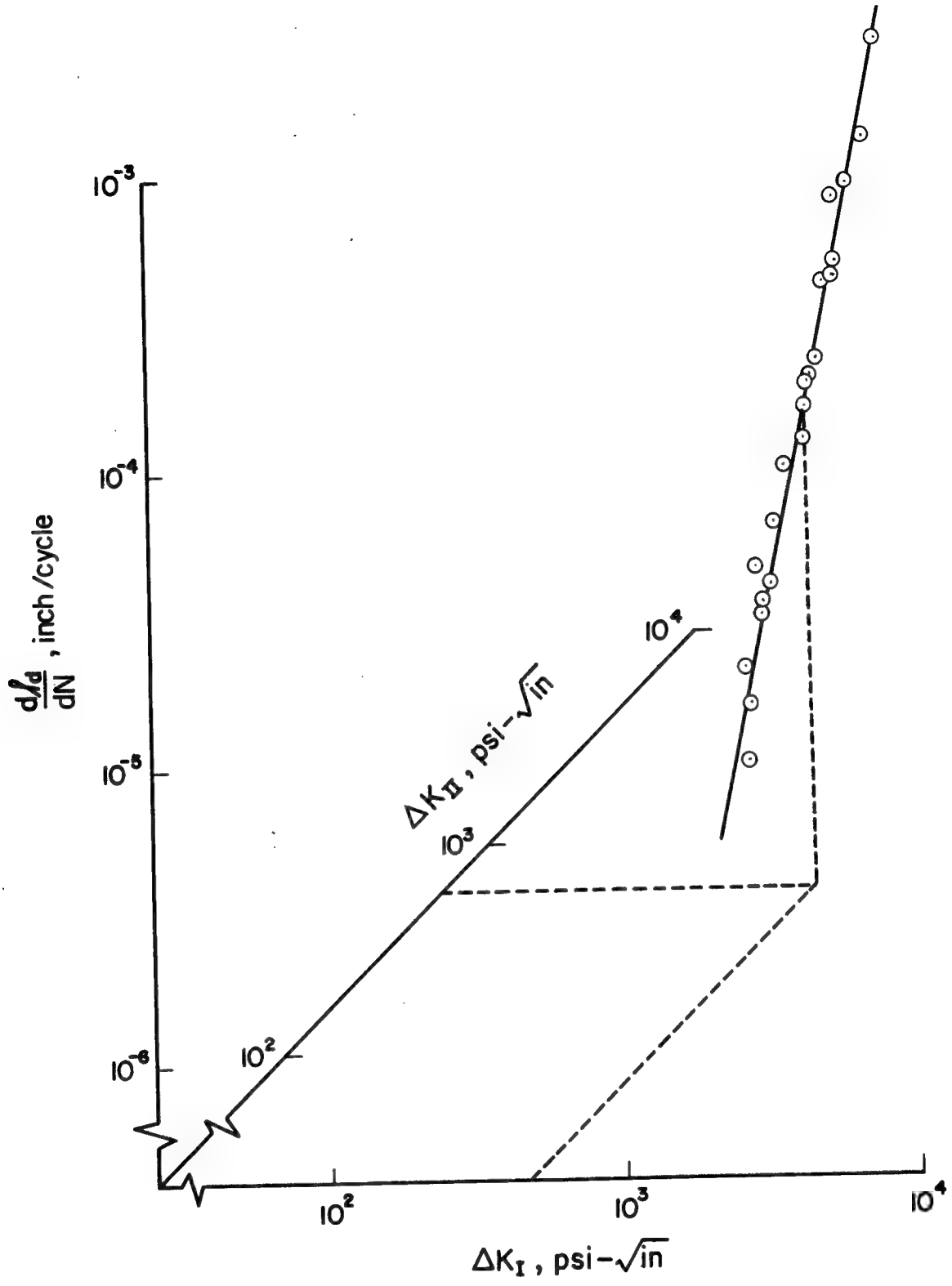

FIG. 11 INTERLAMINAR CRACK GROWTH RATE dl_d/dN AS A FUNCTION OF MIXED-MODE STRESS FACTOR RANGES ΔK_I & ΔK_{II} FOR (0%0%//0%/0%/0%/0%/0%/0°) GLASS/EPOXY

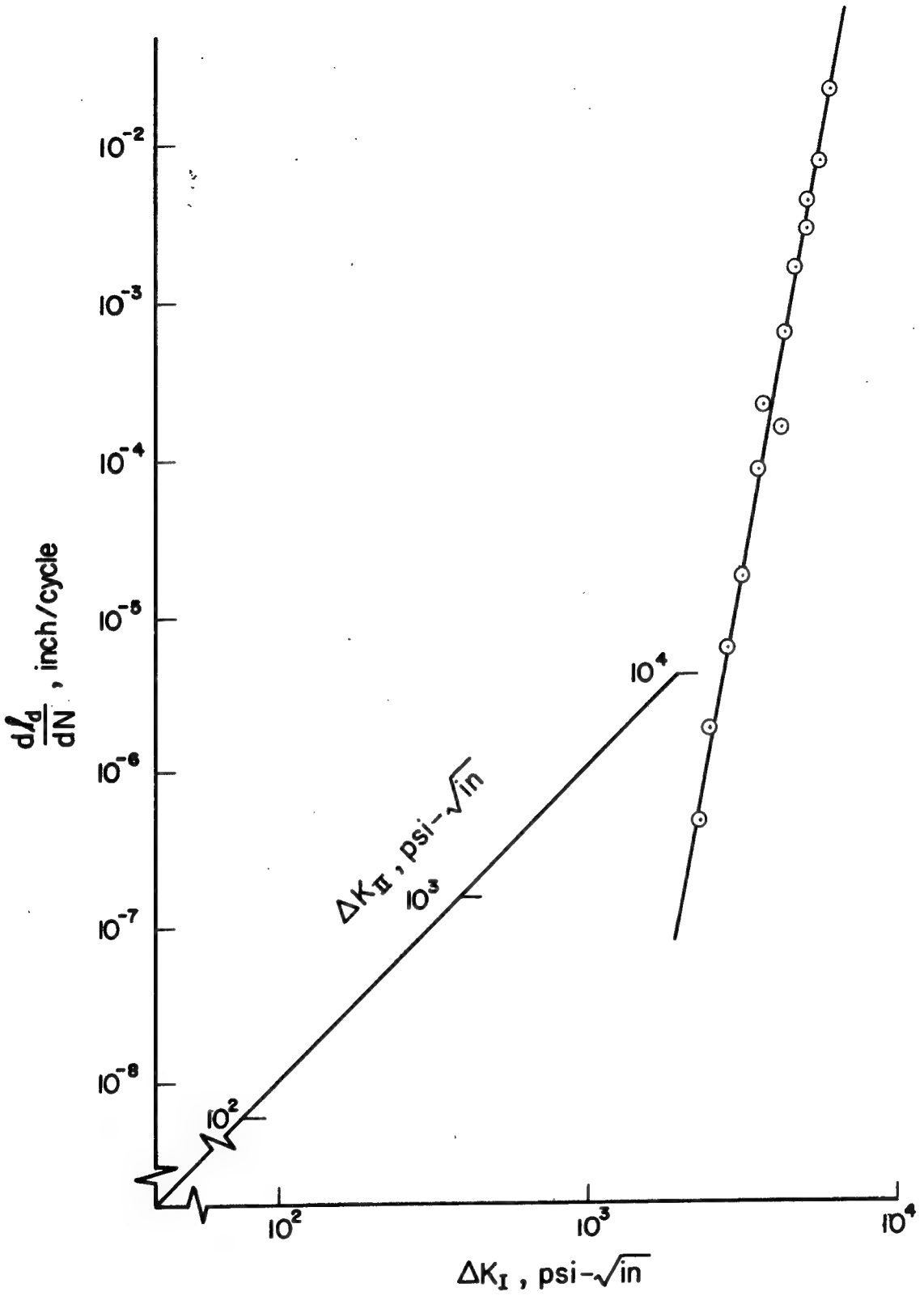

FIG. 12 INTERLAMINAR CRACK GROWTH RATE dl_d/dN AS A FUCTION OF RANGES OF MIXED-MODE STRESS INTENSITY FACTORS, ΔK_I & ΔK_{II} FOR (45%-45%/45%-45%-45%/45%-45%/45°) GLASS/EPOXY

FINAL REPORT PART III - DISTRIBUTION LIST

NSG3044

INTERLAMINAR CRACK GROWTH IN
FIBER REINFORCED COMPOSITES DURING FATIGUE
NASA CR-165434

Advanced Research Projects Agency
Washington DC 20525
Attn: Library

Advanced Technology Center, Inc.
LTV Aerospace Corporation
P.O. Box 6144
Dallas, TX 75222
Attn: D. H. Petersen
W. J. Renton

Air Force Flight Dynamics Laboratory
Wright-Patterson Air Force Base, OH 45433
Attn: E. E. Baily
G. P. Sendeckyj (FBC)
R. S. Sandhu

Air Force Materials Laboratory
Wright-Patterson Air Force Base, OH 45433
Attn: H. S. Schwartz (LN)
T. J. Reinhart (MBC)
G. P. Peterson (LC)
E. J. Morrisey (LAE)
S. W. Tsai (MBM)
N. J. Pagano
J. M. Whitney (MBM)

Air Force Office of Scientific Research
Washington DC 20333
Attn: J. F. Masi (SREP)

Air Force Office of Scientific Research
1400 Wilson Blvd.
Arlington, VA 22209

AFOSR/NA
Bolling AFB, DC 20332
Attn: A. K. Amos

Air Force Rocket Propulsion Laboratory
Edwards, CA 93523
Attn: Library

Babcock & Wilcox Company
Advanced Composites Department
P.O. Box 419
Alliance, Ohio 44601
Attn: P. M. Leopold

Bell Helicopter Company
P.O. Box 482
Ft. Worth, TX 76101
Attn: H. Zinberg

The Boeing Company
P. O. Box 3999
Seattle, WA 98124
Attn: J. T. Hoggatt, MS. 88-33
T. R. Porter

The Boeing Company
Vertol Division
Morton, PA 19070
Attn: E. C. Durchlaub

Battelle Memorial Institute
Columbus Laboratories
505 King Avenue
Columbus, OH 43201
Attn: L. E. Hulbert

Bendix Advanced Technology Center
9140 Old Annapolis Rd/Md. 108
Columbia, MD 21045
Attn: O. Hayden Griffin

Brunswick Corporation
Defense Products Division
P. O. Box 4594
43000 Industrial Avenue
Lincoln, NE 68504
Attn: R. Morse

Celanese Research Company
86 Morris Ave.
Summit, NJ 07901
Attn: H. S. Kliger

Commander
Natick Laboratories
U. S. Army
Natick, MA 01762
Attn: Library

Commander
Naval Air Systems Command
U. S. Navy Department
Washington DC 20360
Attn: M. Stander, AIR-43032D

Commander
Naval Ordnance Systems Command
U.S. Navy Department
Washington DC 20360
Attn: B. Drimmer, ORD-033
M. Kinna, ORD-033A

Cornell University
Dept. Theoretical & Applied Mech.
Thurston Hall
Ithaca, NY 14853
Attn: S. L. Phoenix

Defense Metals Information Center
Battelle Memorial Institute
Columbus Laboratories
505 King Avenue
Columbus, OH 43201

Department of the Army
U.S. Army Aviation Materials Laboratory
Ft. Eustis, VA 23604
Attn: I. E. Figge, Sr.
Library

Department of the Army
U.S. Army Aviation Systems Command
P.O. Box 209
St. Louis, MO 63166
Attn: R. Vollmer, AMSAV-A-UE

Department of the Army
Plastics Technical Evaluation Center
Picatinny Arsenal
Dover, NJ 07801
Attn: H. E. Pebly, Jr.

Department of the Army
Watervliet Arsenal
Watervliet, NY 12189
Attn: G. D'Andrea

Department of the Army
Watertown Arsenal
Watertown, MA 02172
Attn: A. Thomas

Department of the Army
Redstone Arsenal
Huntsville, AL 35809
Attn: R. J. Thompson, AMSMI-RSS

Department of the Navy
Naval Ordnance Laboratory
White Oak
Silver Spring, MD 20910
Attn: R. Simon

Department of the Navy
U.S. Naval Ship R&D Laboratory
Annapolis, MD 21402
Attn: C. Hersner, Code 2724

Director
Deep Submergence Systems Project
6900 Wisconsin Avenue
Washington DC 20015
Attn: H. Bernstein, DSSP-221

Director
Naval Research Laboratory
Washington DC 20390
Attn: Code 8430
I. Wolock, Code 8433

Drexel University
32nd and Chestnut Streets
Philadelphia, PA 19104
Attn: P. C. Chou

E. I. DuPont DeNemours & Co.
DuPont Experimental Station
Wilmington, DE 19898
Attn: D. L. G. Sturgeon

Fiber Science, Inc.
245 East 157 Street
Gardena, CA 90248
Attn: E. Dunahoo

General Dynamics
P.O. Box 748
Ft. Worth, TX 76100
Attn: D. J. Wilkins
Library

General Dynamics/Convair
P.O. Box 1128
San Diego, CA 92112
Attn: J. L. Christian
R. Adsit

General Electric Co.
Evendale, OH 45215
Attn: C. Stotler
R. Ravenhall

General Motors Corporation
Detroit Diesel-Allison Division
Indianapolis, IN 46244
Attn: M. Herman

Georgia Institute of Technology
School of Aerospace Engineering
Atlanta, GA 30332
Attn: L. W. Rehfield

Grumman Aerospace Corporation
Bethpage, Long Island, NY 11714
Attn: S. Dastin
J. B. Whiteside

Hamilton Standard Division
United Aircraft Corporation
Windsor Locks, CT 06096
Attn: W. A. Percival

Hercules, Inc.
Allegheny Ballistics Laboratory
P. O. Box 210
Cumberland, MD 21053
Attn: A. A. Vicario

Hughes Aircraft Company
Culver City, CA 90230
Attn: A. Knoell

Illinois Institute of Technology
10 West 32 Street
Chicago, IL 60616
Attn: L. J. Broutman

IIT Research Institute
10 West 35 Street
Chicago, IL 60616
Attn: I. M. Daniel

Jet Propulsion Laboratory
4800 Oak Grove Drive
Pasadena, CA 91103
Attn: Library

Lawrence Livermore Laboratory
P.O. Box 808, L-421
Livermore, CA 94550
Attn: T. T. Chiao
E. M. Wu

Lehigh University
Institute of Fracture &
Solid Mechanics
Bethlehem, PA 18015
Attn: G. C. Sih

Lockheed-Georgia Co.
Advanced Composites Information Center
Dept. 72-14, Zone 402
Marietta, GA 30060
Attn: T. M. Hsu

Lockheed Missiles and Space Co.
P.O. Box 504
Sunnyvale, CA 94087
Attn: R. W. Fenn

Lockheed-California
Burbank, CA 91503
Attn: J. T. Ryder
K. N. Lauraitis
J. C. Ekvall

McDonnell Douglas Aircraft Corporation
P.O. Box 516
Lambert Field, MS 63166
Attn: J. C. Watson

McDonnell Douglas Aircraft Corporation
3855 Lakewood Blvd.
Long Beach, CA 90810
Attn: L. B. Greszczuk

Material Sciences Corporation
1777 Walton Road
Blue Bell, PA 19422
Attn: B. W. Rosen

Massachusetts Institute of Technology
Cambridge, MA 02139
Attn: F. J. McGarry
J. F. Mandell
J. W. Mar

NASA-Ames Research Center
Moffett Field, CA 94035
Attn: Dr. J. Parker
Library

NASA-Flight Research Center
P.O. Box 273
Edwards, CA 93523
Attn: Library

NASA-George C. Marshall Space Flight Center
Huntsville, AL 35812
Attn: C. E. Cataldo, S&E-ASTN-MX
Library

NASA-Goddard Space Flight Center
Greenbelt, MD 20771
Attn: Library

NASA-Langley Research Center
Hampton, VA 23365
Attn: J. H. Starnes
J. G. Davis, Jr.
M. C. Card
J. R. Davidson

NASA-Lewis Research Center
21000 Brookpark Road, Cleveland, OH 44135

Attn: Contracting Officer, MS 501-11
Tech. Report Control, MS 5-5
Tech. Utilization, MS 3-16
AFSC Liaison, MS 501-3
S&MTD Contract Files, MS 49-6
L. Berke, MS 49-6
N. T. Saunders, MS 49-1
R. F. Lark, MS 49-6
J. A. Ziemianski, MS 49-6
R. H. Johns, MS 49-6
C. C. Chamis, MS 49-6 (8 copies)
R. L. Thompson, MS 49-6
T. T. Serafini, MS 49-1
Library, MS 60-3 (2 copies)

NASA-Lyndon B. Johnson Space Center
Houston, TX 77001
Attn: S. Glorioso, SMD-ES52
Library

NASA Scientific and Tech. Information Facility
P.O. Box 8757
Balt/Wash International Airport, MD 21240
Attn: Acquisitions Branch (15 copies)

National Aeronautics & SpaceAdministration
Office of Advanced Research & Technology
Washington DC 20546
Attn: L. Harris, Code RTM-6
M. Greenfield, Code RTM-6
D. J. Weidman, Code RTM-6

National Aeronautics & Space Administration
Office of Technology Utilization
Washington DC 20546

National Bureau of Standards
Eng. Mech. Section
Washington DC 20234
Attn: R. Mitchell

National Science Foundation
Engineering Division
1800 G. Street, NW
Washington DC 20540
Attn: Library

Northrop Corporation Aircraft Group
3901 West Broadway
Hawthorne, CA 90250
Attn: R. M. Verette
G. C. Grimes

Pratt & Whitney Aircraft
East Hartford, CT 06108
Attn: J. M. Woodward

Raytheon Co., Missile System Division
Mechanical Systems Laboratory
Bedford, MA
Attn: P. R. Digiovanni

Rensselaer Polytechnic Institute
Troy, NY 12181
Attn: R. Loewy

Rockwell International
Los Angeles Division
International Airport
Los Angles, CA 90009
Attn: L. M. Lackman
D. Y. Konishi

Sikorsky Aircraft Division
United Aircraft Corporation
Stratford, CT 06602
Attn: Library

Southern Methodist University
Dallas, TX 75275
Attn: R. M. Jones

Space & Missile Systems Organization
Air Force Unit Post Office
Los Angeles, CA 90045
Attn: Technical Data Center

Structural Composites Industries, Inc.
6344 N. Irwindale Avenue
Azusa, CA 91702
Attn: R. Gordon

Texas A&M
Mechanics & Materials Research Center
College Station, TX 77843
Attn: R. A. Schapery
Y. Weitsman

TRW, Inc.
23555 Euclid Avenue
Cleveland, OH 44117
Attn: I. J. Toth

Union Carbide Corporation
P. O. Box 6116
Cleveland, OH 44101
Attn: J. C. Bowman

United Technologies Research Center
East Hartford, CT 06108
Attn: R. C. Novak
Dr. A. Dennis

University of Dayton Research Institute
Dayton, OH 45409
Attn: R. W. Kim

University of Delaware
Mechanical & Aerospace Engineering
Newark, DE 19711
Attn: B. R. Pipes

University of Illinois
Department of Theoretical & Applied Mechanics
Urbana, IL 61801
Attn: S. S. Wang

University of Oklahoma
School of Aerospace Mechanical & Nuclear Engineering
Norman, OK 73069
Attn: C. W. Bert

University of Wyoming
College of Engineering
University Station Box 3295
Laramie, WY 82071
Attn: D. F. Adams

U. S. Army Materials & Mechanics Research Center
Watertown Arsenal
Watertown, MA 02172
Attn: E. M. Lenoe
D. W. Oplinger

V.P. I. and S. U.
Dept. of Eng. Mech.
Blacksburg, VA 24061
Attn: R. H. Heller
H. J. Brinson
C. T. Herakovich
K. L. Reifsnider